Alternating Gradient Synchrotron Department
Relativistic Heavy Ion Collider Project
BROOKHAVEN NATIONAL LABORATORY
Upton, New York 11973

Spin Note

AGS/RHIC/SN No. 033

The Comparison of the 3D Field Calculation with the Actual Measurement in the 140 Deg. Helical Model Magnet

Masahiro Okamura

August 9, 1996

For Internal Distribution Only

THE COMPARISON OF THE 3D FIELD CALCULATION WITH THE ACTUAL MEASUREMENT IN THE 140 DEG. HELICAL MODEL MAGNET.

Masahiro Okamura

Last year, a part of slotted type helical dipole magnet was fabricated at BNL, and excitation test was done. I have simulated a model of this magnet using 3D field calculation. In this report, the results of the analysis is presented.

The input method of coil shape.

OPERA-3D was used for the magnetic field calculation of the BNL slotted type helical model magnet. I adopted the input method called "BR20" to describe arrangements and shapes of the conductors in 3D space. In this method a 6 faced body is expressed by the coordinates of 8 corners and 12 middle point between each corner, and each line defining the 6 faces is expressed by a parabolic curve. The model magnet has a pair of 5 slots, upper coils and lower coils. In this calculation each slot was divided into about 80 bricks, 40 pieces in the helical section and approximately 40 pieces in the end section. The whole magnet was divided into 860 parts and the each piece was described by BR20.

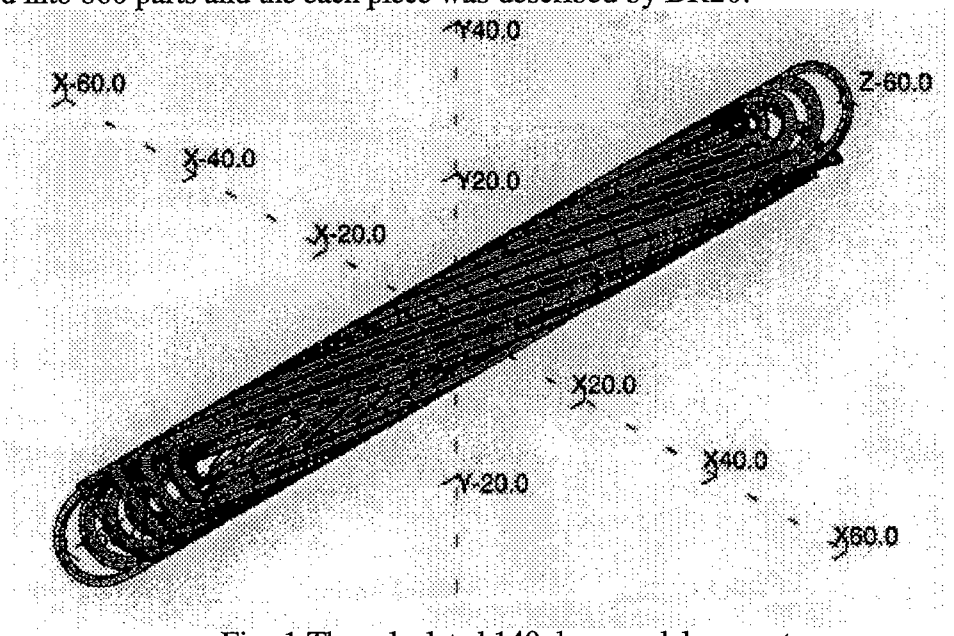

Fig. 1 The calculated 140 deg. model magnet.

The total twist angle of the magnet is 140 deg. and the inner bore radius is 50 mm. In my analysis the depth of slot filled by conductors was set at 8.06 mm which corresponds to 7 layered cables. The flowing current in each cable was set as 382 A. To describe the coil shape at the end region, I used the table created by Dr. Morgan. Therefore the end structure used in my calculation is different from the actual tested model. Figure 1 shows the whole magnet drawn by OPERA-3D.

Maximum magnetic field strength.

The movement of the conductors due to magnetic field causes quenches. It is therefore useful in the design to ascertain where the strongest magnetic field occurs in a magnet. I surveyed the most susceptible positions in this model and found 22800 Gauss around the inner surface of the coil at the end region which is at 52.7 mm from the beam axis. This value is about 1.7 times of 13570 Gauss of the field strength at the center of magnet. This position is pointed in Fig. 2 and 3. At this point the direction of the magnetic field points toward the beam axis (Y component of the field is 22600 Gauss).

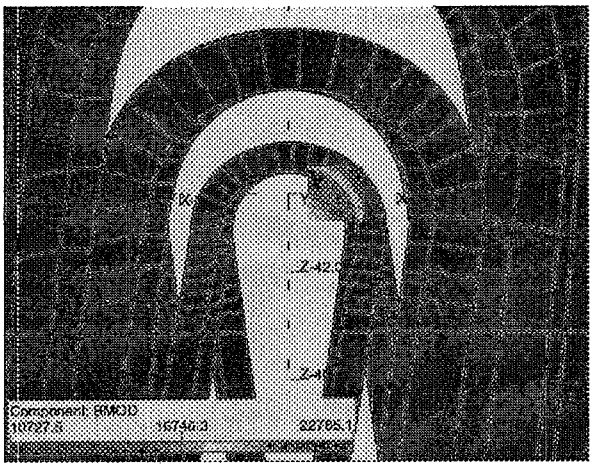

Fig. 2 The end view from up side.

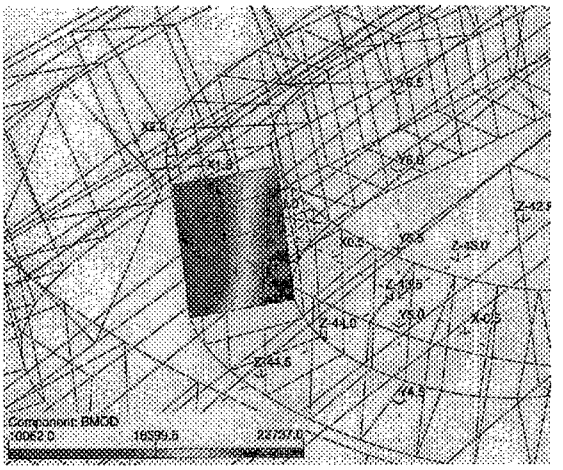

Fig. 3 The field strength at crosssection of the coil

Magnetic field distribution.

The calculated field distributions are shown in Fig. 4 and 5. At off axis position, strong longitudinal fields are expected.

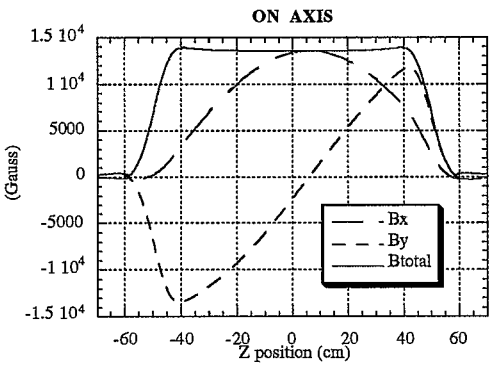

Fig. 4 Field distribution on the beam axis

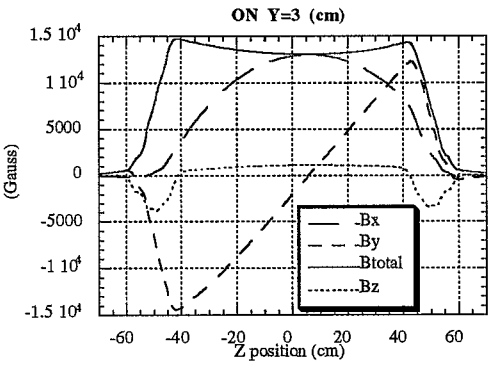

Fig. 5 Field distribution above 3.0 cm from the axis

Comparison with the measurement data of multipole coefficients.

The comparison of measured multipole coefficients with the results calculated by OPERA-3D are shown in several figures at the end of this report. Each value was found by Fourier analysis of measured and calculated azimuthal fields along the circle at a distance of 2.24 cm from axis. The reference radius of Fourier expansion is 2.5 cm. The measured sextupole coefficient is 1.8 times larger than calculated coefficient.

Conclusion

I calculated 3D field and found that the strongest field point in this magnet locates at inside surface of the coil in the end region. The end shape of actual model is different from the calculated model, yet it is expected that the end part was the severest place against quench with a real model. There are strong longitudinal fields which might affect spin motion especially at both ends of the magnet. The longitudinal component of the magnetic field was not measured in the actual model test, however it is strongly recommended in future experiment to measure this component of the field. The cause of difference between the measured and predicted sextupole coefficients is not clear, and the investigation is still in progress.

Acknowledgment

I wish to thank G. Morgan, R. Gupta, A. Jain and E. Willen for information about BNL helical model magnet, also grateful to F. Mariam for discussions and reading this manuscript.

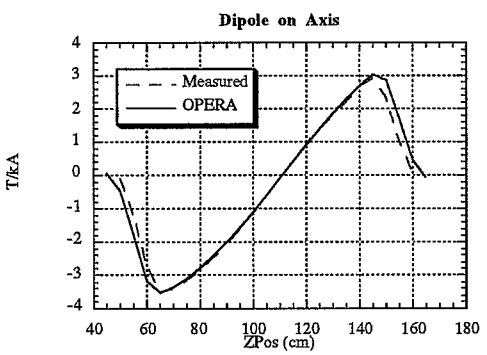

Fig. 6 Dipole component on the axis.

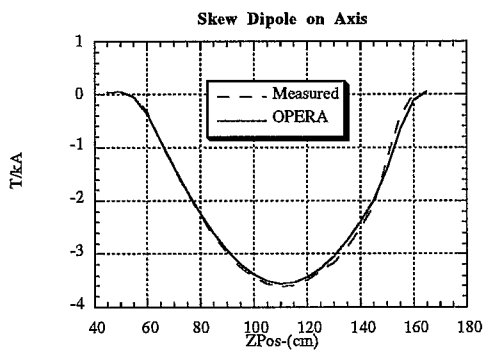

Fig. 7 Skew dipole component on the axis.

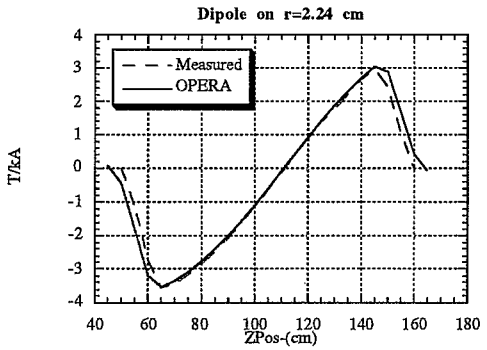

Fig. 8 Dipole component on r=2.24 cm.

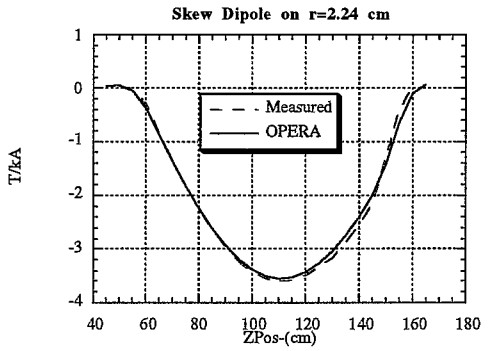

Fig. 9 Skew dipole comp. on r=2.24 cm.

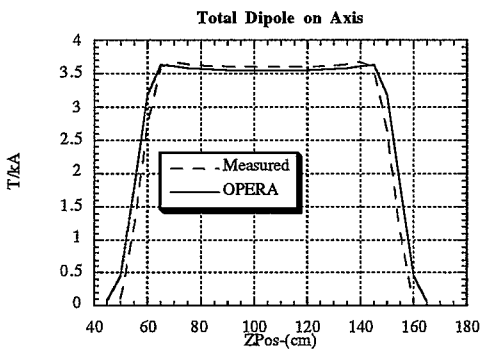

Fig. 10 Total dipole field on the axis.

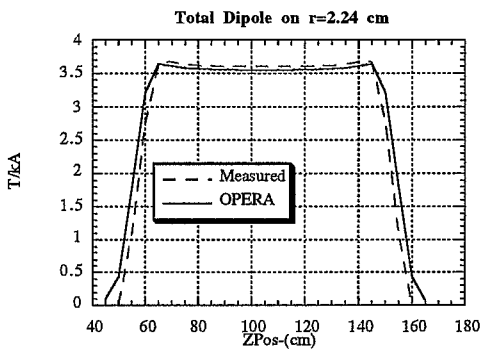

Fig. 11 Total dipole field on r=2.24 cm.

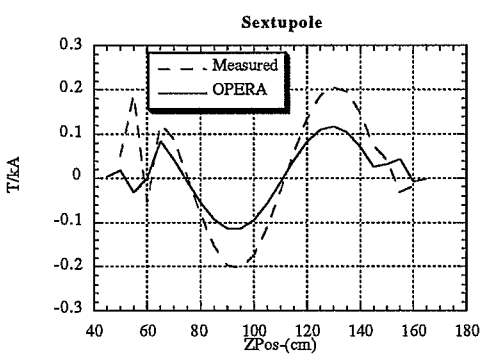

Fig. 12 Sextupole component.

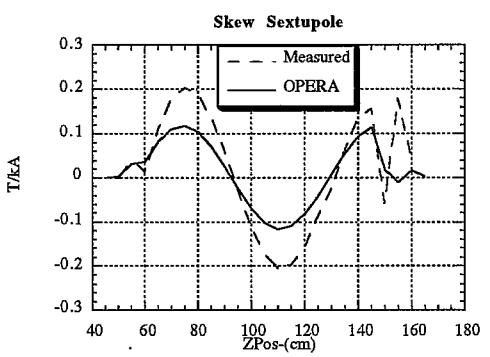

Fig. 13 Skew sextupole component.

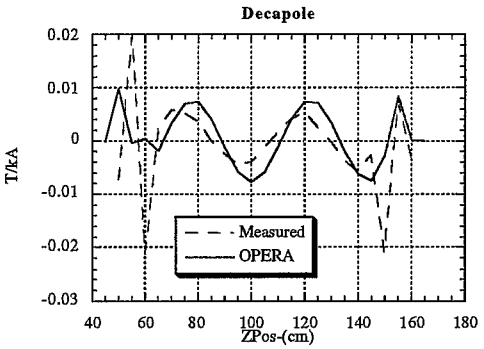

Fig. 14 Decapole component.

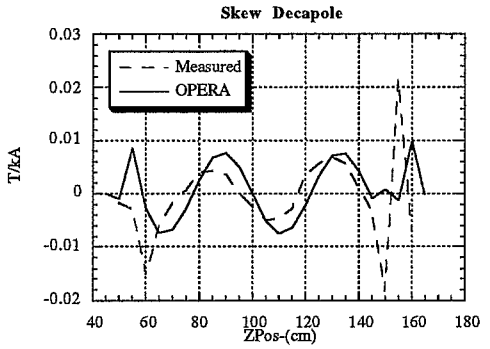

Fig. 15 Skew decapole component.

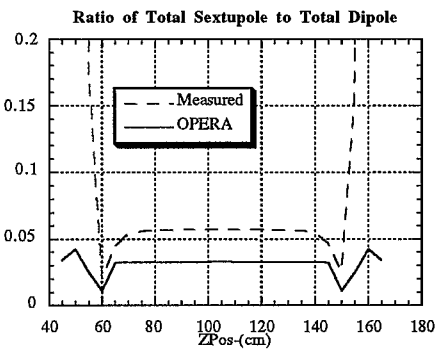

Fig. 16 Ratio of the total sextupole field to the total dipole field.

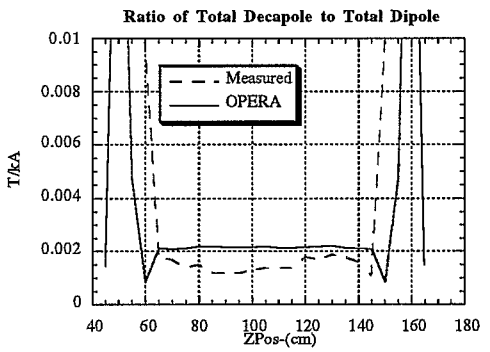

Fig. 17 Ratio of the total decapole field to the total dipole field.